

Morphotectonic Identification Utilizing Satellite Imagery Processing on the Southern Part of Merapi Mount in Yogyakarta

Herry Riswandi^a, Emi Sukiyah^b, Boy Yoseph C.S.S. Syah Alam^{c,1}, Muhamad Sapari Dwi Hadian^{c,2}

^a *Geological Postgraduate Program, Universitas Padjadjaran, Jl. Raya Bandung Sumedang, Jatinangor, Indonesia*
E-mail: herry.riswandi@unpyk.ac.id

^b *Geological Science Department, Universitas Padjadjaran, Jl. Raya Bandung Sumedang, Jatinangor, Indonesia*
E-mail: emi.sukiyah@unpad.ac.id

^c *Applied Geology Department, Universitas Padjadjaran, Jl. Raya Bandung Sumedang, Jatinangor, Indonesia*
E-mail: ¹boy.yoseph@unpad.ac.id; ²sapari@unpad.ac.id

Abstract — This study investigates the relation between morphological spatial orientation features, lineaments trends and geological structures in the southern slope of Merapi Mountain in Yogyakarta, Indonesia. Digital processing using Landsat 8 OLI/TIRS and digital elevation model data 30 m resolution to construct and extract automatically identifying structure lineaments and stream network. Azimuth frequency and length density distribution analyze from morphological features. Geological structure controls the landscape were analyzed use profile data from the southerly flowing stream. The structure trends north-south were profiles taken with the topo-relief changes between the slightly gradient and the depth of mountain front in the part of the south mountain slope. Dendritic-trellis stream modification types show different anomaly along surface stream profile intersects with fault and lineaments. Azimuth lineaments analysis indicating north-south, east-west, northeast-southwest, and northwest-southeast trends compared with stream surface flow system, the direction classification show similarity structures control trends in the geomorphological surface. These lineament structures provide cannellure for surface water flow. The lineaments form extraction divided into three population bases on an outcrop of the host rock, to getting information of geologic time trend evolution. Lineament trend spread into different lithology because of tectonic activity from the weak zone of surface discontinuity from the recent surface landscape.

Keywords — geological structure; geomorphological; digital processing; Landsat 8; digital elevation model.

I. INTRODUCTION

Merapi Mountain in Java Island, Indonesia, is the most active volcanoes in Asia, implicating geological shifting, tectonic and morphologic stages, that lies in a complex interaction zone between Eurasia, Australia, and Pacific lithospheric plates [1]. Merapi volcanic area is one of the pull-apart basins in Java Island because of this tectonic implication, and the volcanic evolution interpretation base on the active Opak-Prambanan Fault [2] and Muria Fault [3], [4] with NE-SW lineament direction (Fig. 1). The implication of the volcanic deformation produced geologic structures on the various geologic ages, and it related to geomorphological aspects as valleys and sloped discontinuation on the surface [5]–[7].

Satellite imaging utilized for quick deformation process identification, extraction and structure lineament using suitable software, because it is efficient and faster than a manual process [8][9]. Lineament identification it will be difficult if it only depended on geological fieldwork. An

automatic extraction has an obstacle to distinguish geological lineaments or beside geological structure such as railway and irrigation channel [10]–[12].

However, many studies are explaining the geological setting of the southern part of Merapi volcano, but it is still unclear detailed report of lineaments and their tectonic activity relationship [13], [14]. This study was an attempt to digital processing by utilized Landsat 8 Operational Land Imager/Thermal Infrared Sensor (OLI/TIRS) and 30-meter ASTER-DEM extract stream flow direction to analyzed recent geological deformation of geological lineaments structure orientation [15].

Stream network used to identifying structural control on the geomorphic configuration on a local scale [16]. Tectonic evidence in Merapi volcanic is an exciting place for tectonic deformation studies because it has preferential variety geomorphology evolution Tertiary-Quaternary rocks. The primary objective was to evaluate and to identify active tectonics from morphotectonic anomalies where it reflected in the morphology of the landform, lineaments and stream

network from remote sensing and GIS extraction and analysis.

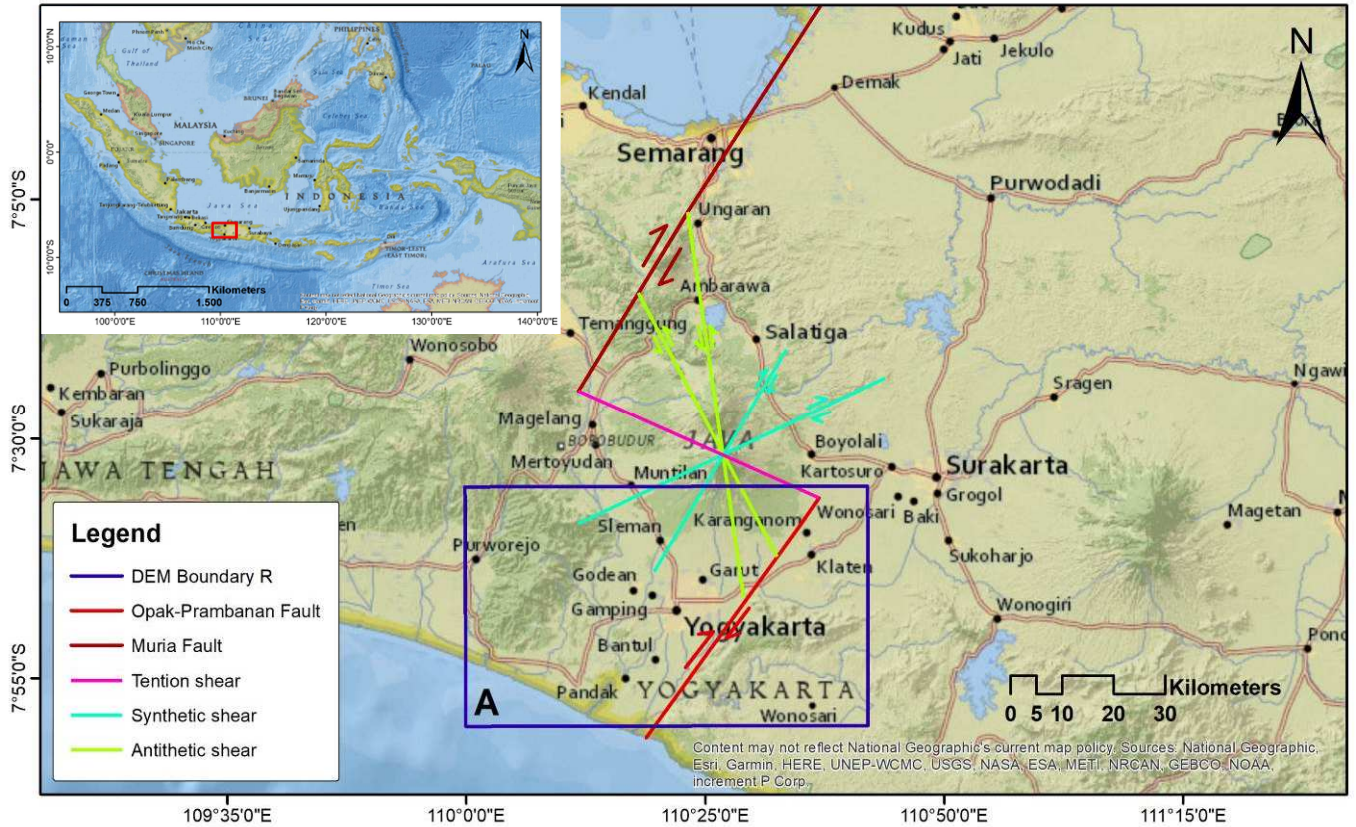


Fig. 1. Map using National Geographic Esri and SRTM 1 Arc-Second Global 30-m DEM with hillshade image analysis 0-45-90-135 altitude combination. The research location is in the southern slope of Merapi Volcanic recharge area, Yogyakarta, Java Island, Indonesia. Geological setting of pull-apart basin center in Merapi Volcano with structure evolution with mayor fault of Opak-Prambanan and Muria lineament and shear of tension, synthetic and antithetic lineament. (A) DEM Boundary of the location of study area.

II. MATERIAL AND METHOD

The location study area is on the southern slope Merapi volcanic mountain covers 3000 km² over an altitude of 0 to 850 m above the sea level. It composed of Tarsier sediment deposit to Quaternary volcanic deposits (Fig. 2).

A. Geological Setting

The Tarsier sediment outcrops are local places that can be found easily in the southeasternmost segment of southern ridges and exposed the oldest rock found in Java Island. These rocks form part of the Eocene-Miocene with the formation of different rock deposits.

The southern mountain regionally lithostratigraphy consisted of the Late Eocene Wungkal composed by metamorphic (schist, phyllite, and marble), igneous (diomite and gabbro) and sediment rocks [17]. The Late Eocene Wungkal rocks sequence uplifted occur with high volcanic activity overlain by Late Oligocene sediment Kebo-Butak. This Oligocene rocks conformity with Semilir and Nglanggran rocks formation of ancient volcanogenic exploitation and constructive lava layer in the Early Miocene [18]. In the Middle Miocene, the volcanic were low activity and composed sediment carbonate Sambipitu with north-south tectonic compression and then uplifted with unconformity carbonate clastic Oyo [19]. Middle Miocene

Oyo inter-fingered with Pliocene carbonate Wonosari and Kepek rocks formation while tectonic uplifted continues [20].

The part of the west side exposed Tarsier volcanic breccia dominated rocks with dome morpho-shape. The west mountain ridges regionally lithostratigraphy were consist of the Eocene sediment carbonate Nanggulan. These Eocene rocks overlay by unconformity Late Oligocene sediment Kebo-Butak and intruded with Oligocene Andesite when it had high volcanic activity and the sea level continuously uprising.

Kebo-Butak rocks formation overlain by unconformity Late Miocene sediment carbonate Jonggrangan in the low volcanic activity phase, it was interfingering with Pliocene carbonate clastic Sentolo influenced with the anticline-syncline fold. For this two area in the east and west of the southern ridges exposed significant outcrop, but in the north, the area is the slope of Merapi volcano very rare to discovering Tarsier outcrop, because of continuously volcano activity period [17], [18], [20].

Rock formation in the slope of Merapi volcanic covered with young to old Merapi volcanic deposits. This volcanic mountain is growing in the middle of a joint point, between E-W and N-S volcanic range lineaments. This deposit increases over time eruption and changes the stream pattern with thick volcanic deposits [21].

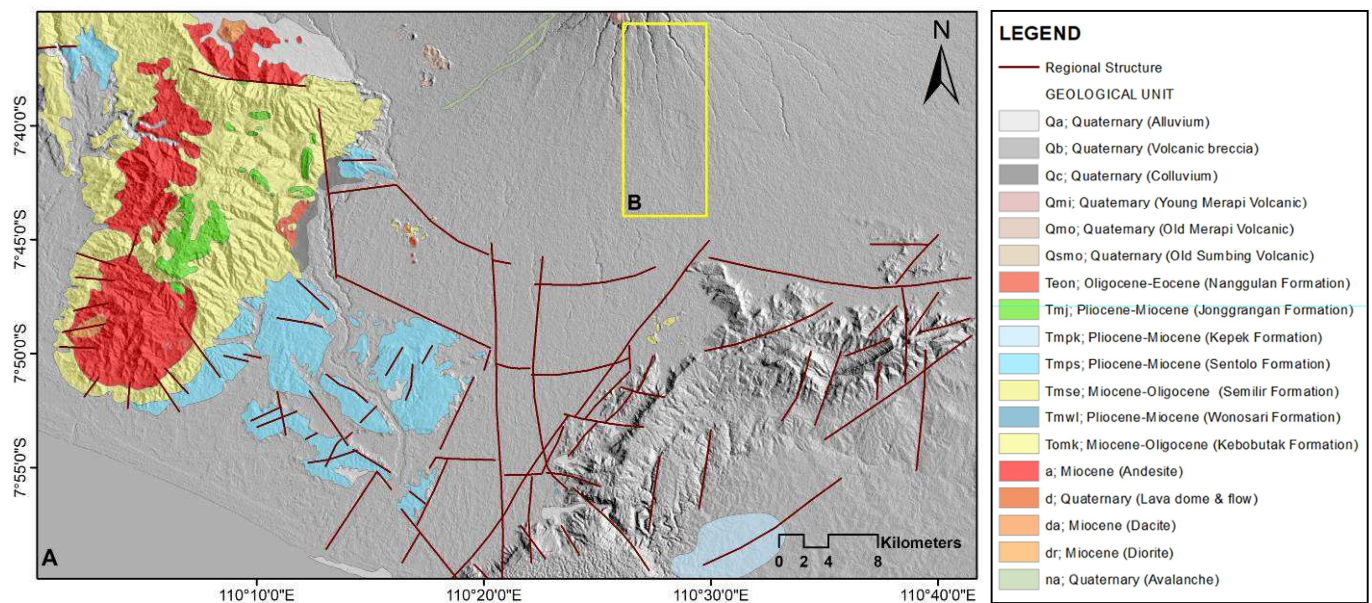


Fig. 2. Geological map with a regional structure of the southern part of Merapi in Yogyakarta. Geological Research and Development Center provided Geological information [22]. (B) Small scale for Hill-shaded images with lighting from various azimuth angle.

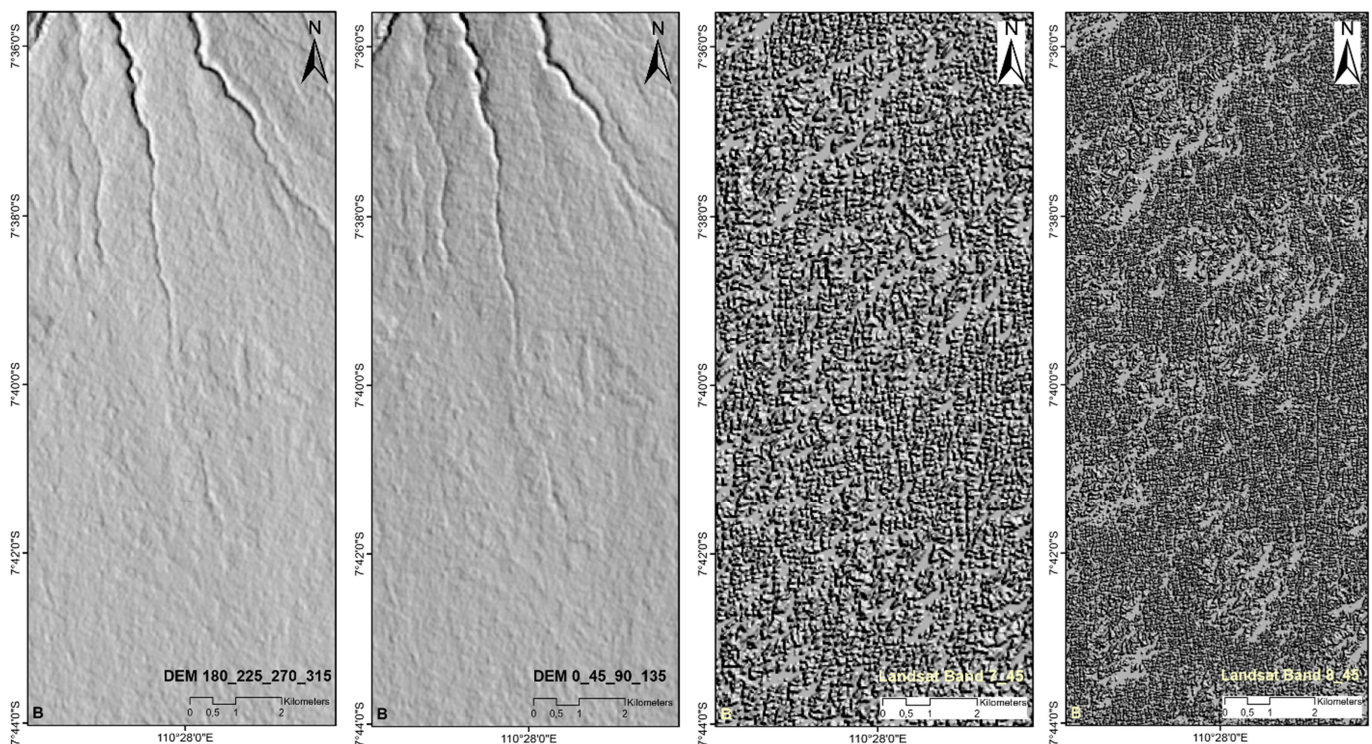


Fig. 3. Hill-shaded image from four directions with lighting from various azimuth angle of 180°-225°-270°-315° for positive relief features and 0°-45°-90°-135° for negative relief features. Landsat 8 band 7 (30 m resolution) and 8 (15 m resolution) with the 45° the light source azimuth angles.

B. Remote Sensing Material

The structural remote sensing analysis of the southern slope of Merapi volcano used the optical and elevation data from the Landsat 8 OLI/TIRS (11 spectral bands) path-row number 120-065. Landsat 8 OLI/TIRS with 30 meters spatial resolution for band 7, and 15 meters spatial resolution for panchromatic band 8. Remote sensing analysis also used Shuttle Radar Topography Mission (SRTM) data with Digital Elevation Model (DEM) format elevation grid one arc-second spatial resolution (30 meters) for latitude 7°-8°,

and longitude 110°-111° in GeoTIFF format were acquired 28th October 2018. These imagery data downloaded from the United States Geological Survey in Earth Explorer portal [23] were Universal Transverse Mercator zone 49-South projected in World Geodetic System 1984 Datum to Geographic Coordinate System.

The elevation data from imagery were resized of the study area using ArcGIS 10.4 digital processing to extract and analyzed lineaments and stream network from hill-shades images [24]. Hill-shades images analysis generally used to

identify tectonic activity orientation. Hill-shades analytical technique used to simulate the artificial effect from all point that has altitude and azimuth illumination. Using different sun azimuth hill-shade image from DEM by application illustrating the visual differences of the linear features identified the light source of the azimuth angle [25].

Method of a directional oblique-weighted (MDOW) shaded relief used ArcGIS computer process to generate the light source different azimuth angle (180°, 255°, 270°, 315° and 0°, 45°, 90°, 135°) combination from DEM (Fig. 3) surface trends hill-shades images and weighted using aspect image [26][27]. This method to aim the comparable of the lineaments generated two different light azimuth combination into a single image provides a linear characteristic related that cannot see clearly if only use one single lighted hill-shades image. The identification of lineaments and lithological was also used Landsat 8 scenes to comparative analysis (band 7 and band 8). PCI geomatic v.17 software to lineaments extraction from imagery [28]. Lineament visual inspection removed that matched artificial

features such as irrigation channel. Lineaments evaluated with their strike, length, and density charted on the rose diagram for directional analysis and to understanding the lineaments spatial distribution.

Stream network is often influencing by the geological structure in the active tectonic area in the different tectonic setting. This network pattern was essential for morphotectonic analysis using GIS software to automatic identification from DEM data [29]. The ArcGIS Toolset extraction to extracted the drainage system including filling, flow direction, density, drainage, and distribution. The direction and length of the stream network were evaluated and illustrated on the rose diagram using spatial GIS operation to the preferred orientation of water flow on the surface [30].

Filed data are necessary to validate surface information of the lineament's analysis, including the strike and dip measuring of fault and fracture and it displayed on the rose diagram to determine dominated orientations.

TABLE I
STATISTICAL CHARACTERISTIC OF MULTI-ILLUMINATION HILL-SHADED IMAGES

Characteristic	DEM		Landsat 8	
	0°, 45°, 90°, 135°	180°, 255°, 270°, 315°	Band 7	Band 8
No. Lineaments	4686	968	1061	4851
Minimal length (m)	306.3	918.8	900	450
Maximal length (m)	4251.8	8027.7	5428.1	3674.7
Total length (km)	2742.4	1757.2	1573.9	3675.4

III. RESULT AND DISCUSSION

The surface relief features revealed a different direction and displayed a stream of the positive and negative section, and it created by combining various light azimuth from two shades images with of 180°-225°-270°-315° and 0°-45°-90°-135° of the light source azimuth (Fig. 3).

The positive relief element represents evaluated topography such as ridges and scarps, and the negative element represents fault, valley, trenches, and joints.

The statistic for 4686 lineaments DEM 1 (0°-45°-90°-135°) population has 2742.4 km total length with 306.3 m for minimum and 4251.8 m for maximum. DEM 2 (180°-225°-270°-315°) have 968 lineaments population for 1757.2 km total length with 918.8 m for minimum and 4251.8 m for maximum. Landsat band 7 have 1061 lineaments population for 1573.9 km total length with 900 m for minimum and 5428.1 m for maximum. Landsat band 8 have 4851 lineaments population for 3675.4 km total length with 450 m for minimum and 3674.7 m for maximum (Table 1). The lineaments population length frequency and weighted distribution projected in the histogram (Fig. 4).

Landsat and DEM hill-shaded extraction images show very different results to Landsat 8 imagery. The DEM lineaments are concentrating on the higher topographic relief density. Imagery result for Landsat band 8 is higher lineament than band seven because of spatial resolution in

band 8 has a 15-meter resolution, and band 7 has a 30-meter resolution.

The direction of azimuth straightness from the four images from DEM and Landsat 8 imagery does not follow the same pattern. The direction of the azimuth lineaments from DEM 1 show almost has a similar rose diagram with band seven that higher concentration in the northeast to southwest; DEM 2 show higher concentration in the northwest to southeast trend. The azimuth lineaments direction Landsat band eight show east-west, north-south, northeast-southwest, and northwest-southeast trend (Fig. 4). The DEM lineament analysis concentrates in Kulonprogo and Gunungkidul Tersier area, and the lineaments in the northern to southern Sleman area are generally rarely extracted because of this area covered by a thick deposit of other Recent volcanic (Fig. 4).

The stream density spatial distribution is applying from the extracted DEM 1 shows the highest concentration of stream along the hills and lineaments Fault. Stream network consisted pattern of a dendritic-parallel-trellis-rectangular and modified dendritic or trellis pattern (Fig. 5).

Measuring 120 faults from different locations on different lithologies spread in four areas on the fields, that are Sleman (southern part slope of Merapi Volcano), Kulonprogo (western part of Sleman area), Gunungkidul (eastern part of Sleman), and Bantul (southern part of Sleman). Fault strike variety recorded with east-west, north-south, northeast-southeast, and northwest-southeast trends, from centimeter to meters.

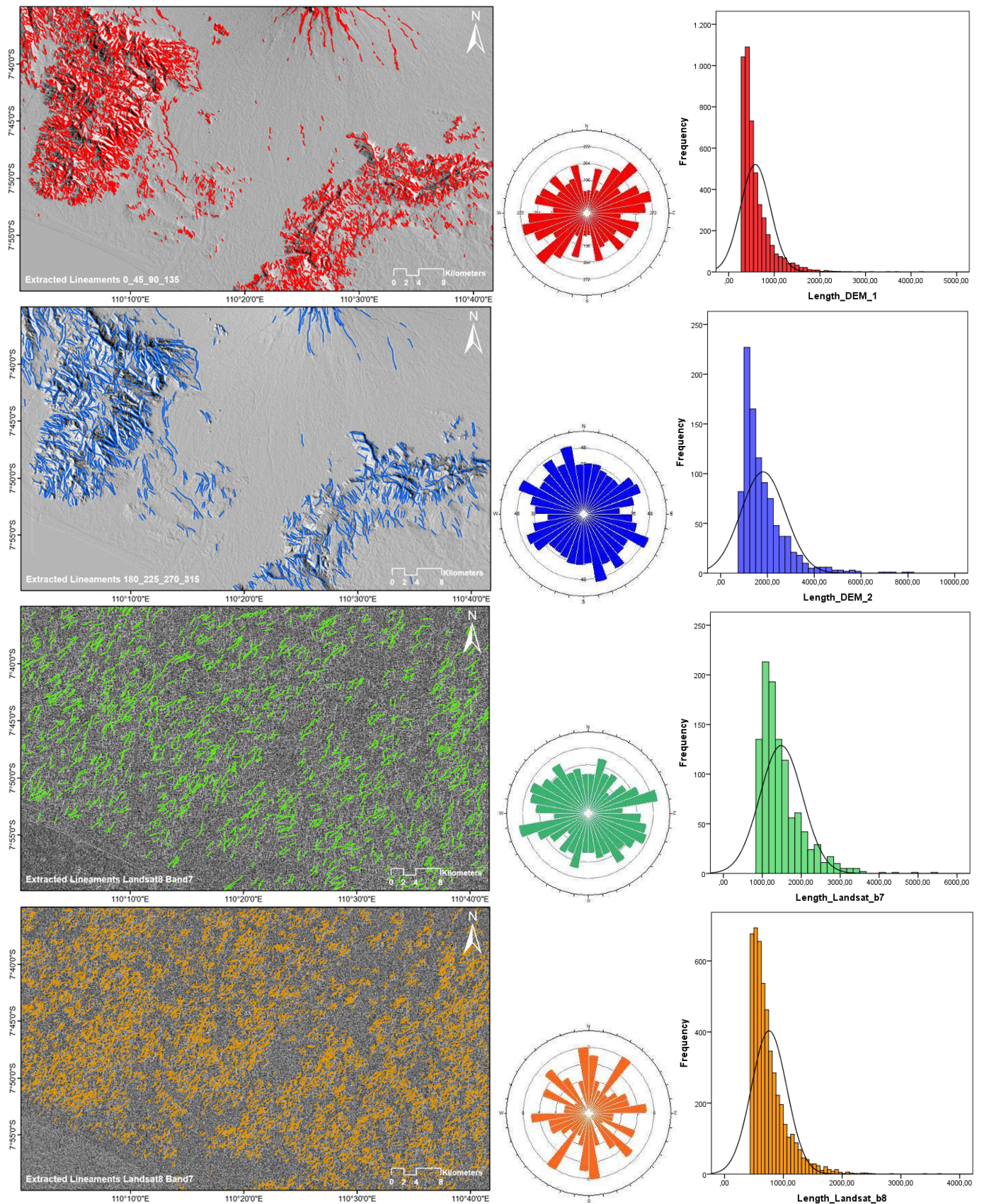


Fig. 4. Imagery from DEM and Landsat 8 imagery analyze different light azimuth of 0° - 45° - 90° - 135° (DEM 1); 180° - 225° - 270° - 315° (DEM2); band 7 and band 8 of Landsat 8. Each lineaments trend differently has its direction with length frequency distribution shows each histogram.

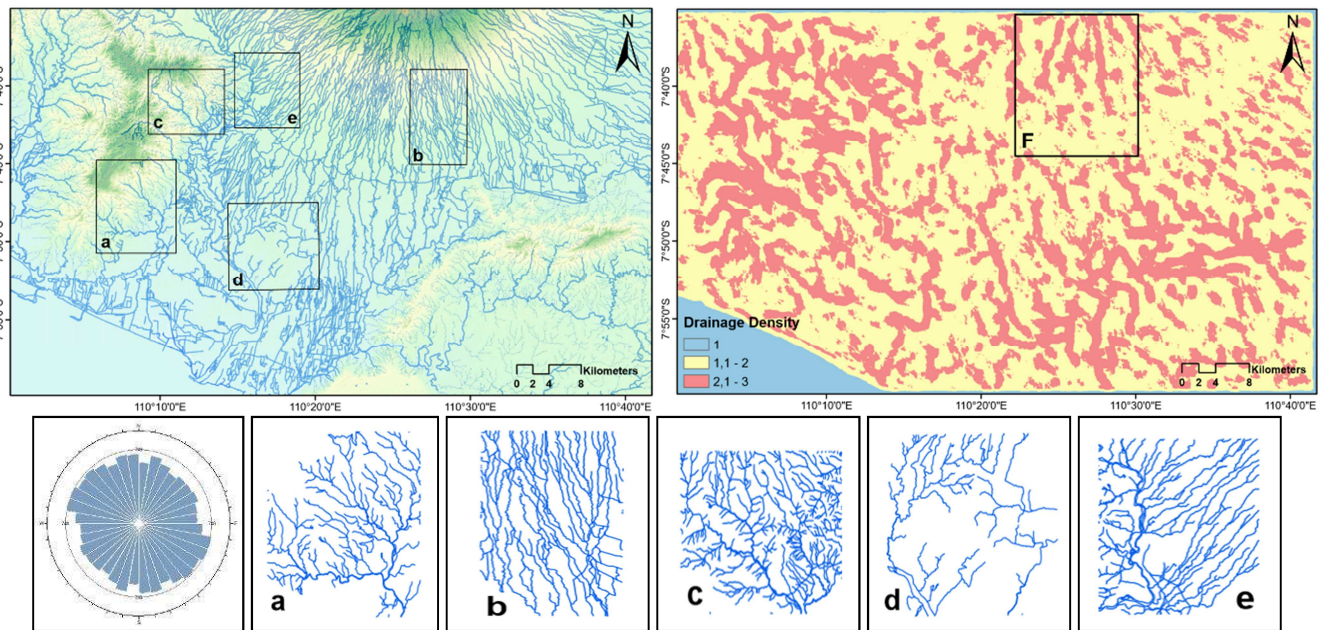


Fig. 5. Flow direction in the drainage system is indicating by a solid blue line derived from DEM with a rose diagram showing direction for surficial water north-east, east-west, northeast-southwest, and northwest-southeast. Drainage density with a 1 km radius showing the pattern of drainage pattern. Drainage pattern recognize as; (a) dendritic, (b) parallel-sub parallel, (c) trellis, (d) rectangular, (e) dendritic to trellis. (F) Valley-floor width to valley height (Vf) cross-sectional stream channel profile in a southern part of Merapi volcano.

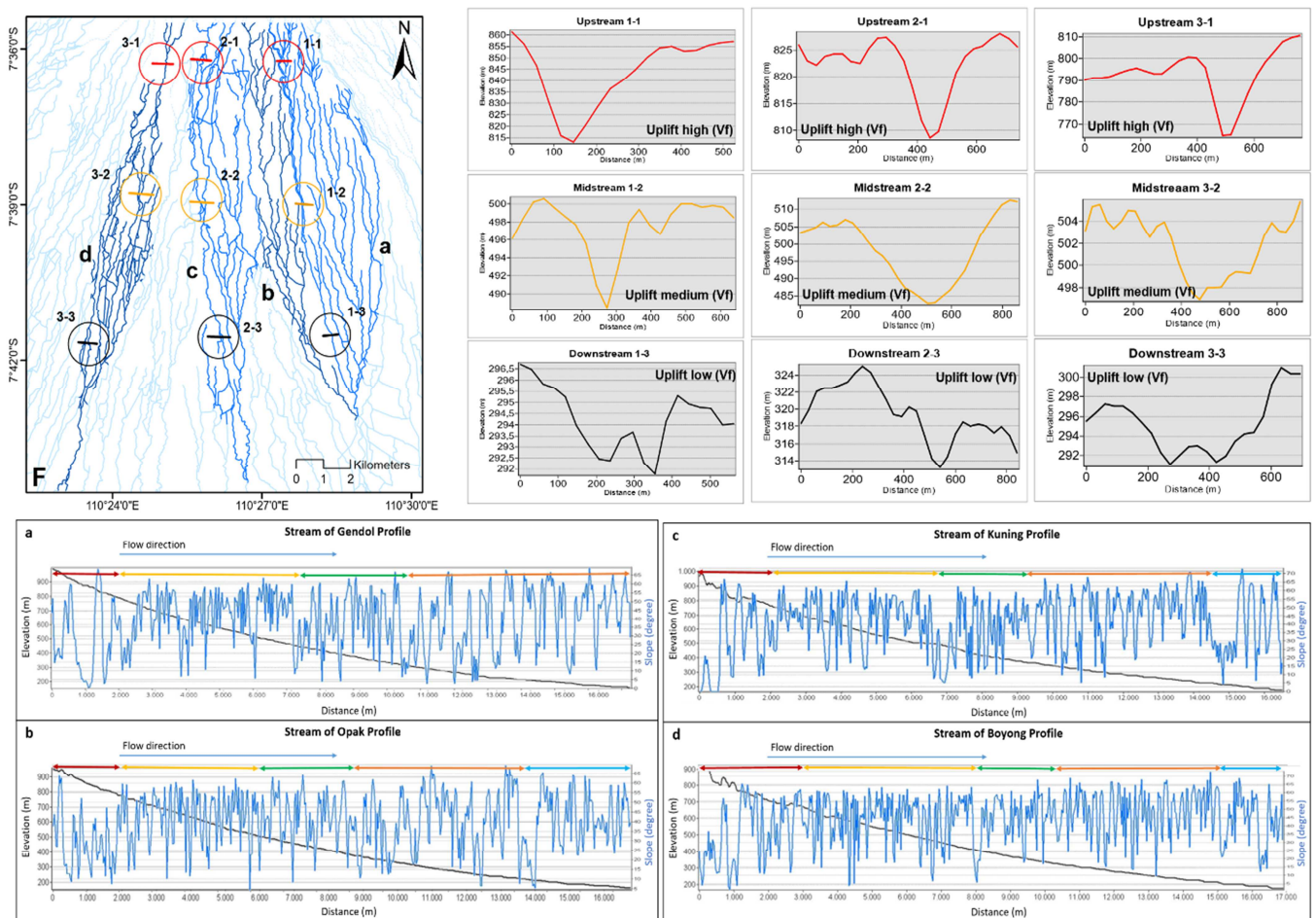


Fig. 6. Cross-sectional stream profiles of four large tributaries recharge area in the southern part of Merapi volcano. Longitudinal profile stream channel of (a) Gendol, (b) Opak, (c) Kuning, and (d) Boyong are generating from 30 m DEM (black and blue line indicate the variation of the elevation and slope degree along the flow direction). The stream indicating tectonic implication (Vf) is high uplifted in the upstream, medium uplifted in the middle stream, and low uplifted in the lower stream.

A. Geomorphological and geological structures

Remote sensing was used to mapping automatically of DEM and Landsat 8 lineaments with each length and direction. The four main orientation for azimuth distribution lineament is north-east, east-west, northeast-southwest, and northwest-southeast, and it is similar to that stream azimuth distribution, although there are a few directions differences (Fig. 4). The lineament of stream azimuth distribution is a path for rain runoff in the surface and act as a storage entrance with the fluvial horizontal and vertical flow interaction. These stream lineament on the relief topography has significant differences in density. The appearance of high lineament density is shown highest area and this area usually represent complex structural deformation, and it contains the fault and fracture system on the surface (Fig. 5).

The relation between lineament trends and subsurface structural features is exposing the rocks variety in the north-east, east-west, northeast-southwest, and northwest-southeast trends. The best azimuth direction has similarity obtain from DEM data, and the regular structural lineament occurs around Sleman, Kulonprogo, Gunungkidul, and Bantul. Many outcrops have non-linear with the lineament azimuth orientation because the outcrop exposure was minimal to recognize the structural features, most probably subsurface buried structure represent, and only appears in landform characteristic structure influence.

B. Drainage pattern

Tectonic deformation can be found the trailer activity in the controlled drainage pattern of the spatial distribution [31]. The drainage pattern is showing pattern changes along active tectonic deformation where active cross fault and different type of rock [32]. The stream pattern in shape dendritic-sub dendritic lines dominant, and consist of channel-oriented by the uniformity of rock resistance to erosion, with significant structure and slope influence (Fig. 5a). Parallel and sub-parallel drainage pattern the stream flow direction is

controlling by the slope degree and structural implication (Fig. 5b). Trellis and rectangular pattern show the network influenced by the fault and joint system (Fig. 5cd).

Stream profiles variation show drainage different points identification that response to stream. Other factors to identify stream profiles are not detail discussed in the present study because stream identification needs a much more detailed study. The longitudinal profile shows a variable curve and gradient (Fig. 6). Gendol Stream is composed of the upstream, middle stream and downstream parted by a very steep point zone in km-2, 7.2, and 10.5, very high slope 65° , and sharp valley. Opak Stream profile shows four-point zone, between km-2, 6, 9 and 13.5, with north-northwest to south-southeast tectonic lineament trend.

Stream Opak is crossing by two of structure lineament trend northwest to southeast and northeast to southwest. The stream gradient becomes smooth at the end of the profile, because of the surface start to flatten pass. Kuning Stream has composed of upper and lower sides supposition, not a smooth curve. The cross-section profile has notice incision appears to change significantly in km-2, 7, 9, and 14.5, very high slope $65-70^\circ$. Boyong Stream is close to the Kuning Stream composed of upstream, midstream and downstream part distinct by steep point zone between km-3, 8, 10.5 and 13, very high slope $65-70^\circ$. The ratio of valley-floor width to valley height (Vf) can establish the uplift level of tectonic activity [6]. In the upstream to the downstream consistently change from high to low uplift along with the elevation.

C. The Tectonic lineaments implication

The characteristic of the southern part of Merapi consists of the different geological unit with different age and lineament structures. The southern part of Merapi also depends on geological maps precision that 1:25.000 scale digital map to detect changes in lineament azimuth of lineaments separated by Tertiary and Quaternary era and it analyzed and showed in the rose diagram (Fig. 7).

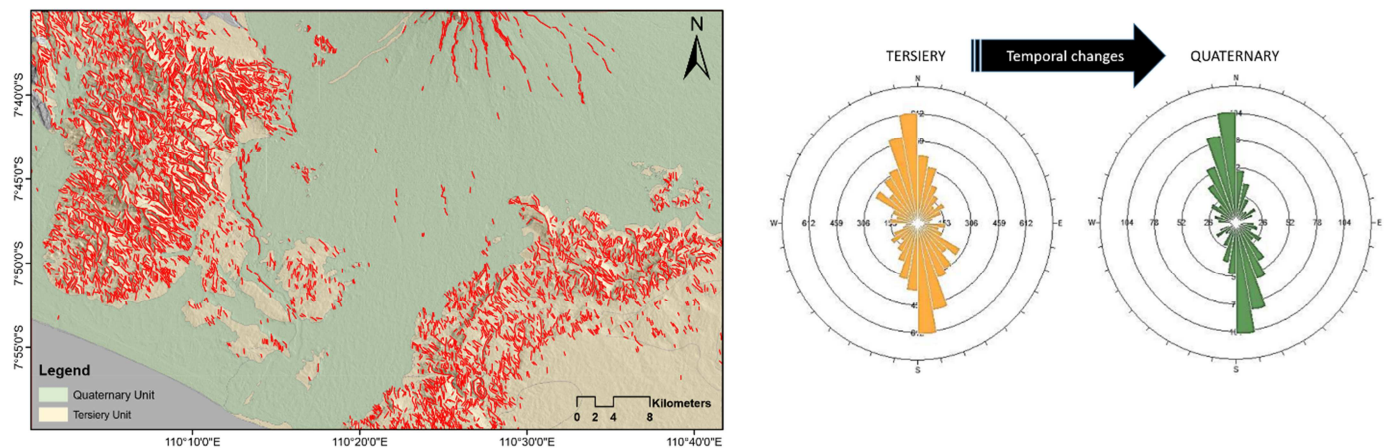


Fig. 7. Lineaments spatial distribution using DEM 30 m through the geologic units with lineaments strike and frequency direction over the rocks unit.

The result shows the lineament has north to south trend azimuth direction dominantly continued from the Tarsier to Quaternary era but in Pre-Tarsier distribution is small detect significantly by GIS data processing. The Quaternary geological structure activity improved the north-northwest to south-southeast azimuth trend most likely associated with a

tectonic activity in the south between Pacific plate and Asian plate based on tectonic activity suggested generated the existing structure reactivation.

Geological structure stress can trigger the most active faults by compressive maximum horizontal stress with northwest to southeast azimuth direction. A major fault with

N30°E strikes parallel to the structure of Opak Fault the dominant system of the north to south lineaments trend interpreted as synthetic shear fractures. The northwest-southeast lineaments trend interpreted as antithetic shear fractures. The west-east acts as tension. The east-west and northeast-southwest lineaments trend as antithetic and synthetic shear (Fig. 1).

IV. CONCLUSION

Remote sensing and GIS analysis technique used to interpret the pattern of the landscape features on the Tarsier to Quaternary age. Resolution of 30 m DEM data, 30 m band 7 and 15 m band 8 of Landsat 8, used to extract their tectonic significance. The hill-shaded analysis used multi-illuminated hill-shading to the determination of the lineament surface features. The hill-shaded analysis which verifying with stream and structure field data changes on the surface. The youngest trend of lineament evolution was north-northwest to the south-southeast, and northwest to southeast, which may be related to reactivation of fault structures during tectonic activity. The stream and structure lineaments in the surface managed or affected by the structure below from the surface.

REFERENCES

- [1] R. W. Van Bemmelen, *The Geology of Indonesia. General Geology of Indonesia and Adjacent Archipelagoes*. 1949.
- [2] I. Nurwidyanto, K. SB, Sismanto, & Waluyo, "The Sub Surface Modeling of Opak Fault Yogyakarta Region with Inversion Method of Gravity Data," *Int. J. Basic Appl. Sci.*, 14, (6), pp. 19–26, 2014.
- [3] J. D. Moody & M. J. Hill, "Wrench-fault tectonics," *Bull. Geol. Soc. Am.*, 67, (9), pp. 1207–1246, 1956, doi: 10.1130/0016-7606(1956)67[1207: WT]2.0.CO;2.
- [4] R. E. Wilcox, T. P. Harding, & D. R. Seely, "Basic Wrench Tectonics," *Am. Assoc. Pet. Geol. Bull.*, 57, (1), pp. 74–96, 1973, doi: 10.1306/819A424A-16C5-11D7-8645000102C1865D.
- [5] E. Sukiyah, E. Sunardi, N. Sulaksana, & P. P. Raditya Rendra, "Tectonic geomorphology of upper Cimanuk Drainage Basin, West Java, Indonesia," *Int. J. Adv. Sci. Eng. Inf. Technol.*, 8, (3), pp. 863–869, 2018, doi: 10.18517/ijaseit.8.3.5441.
- [6] E. Keller, N. Pinter, & D. Green, *Active Tectonics, Earthquakes, Uplift, and Landscape*. New Jersey: Prentice-Hall, 1996.
- [7] J. C. Doornkamp, "Geomorphological approaches to the study of neotectonics," *J. Geol. Soc. London.*, 143, (2), pp. 335–342, 1986, doi: 10.1144/gsjgs.143.2.0335.
- [8] A. B. Ariza-Villaverde, F. J. Jiménez-Hornero, & E. Gutiérrez de Ravé, "Influence of DEM resolution on drainage network extraction: A multifractal analysis," *Geomorphology*, 241, pp. 243–254, 2015, doi: 10.1016/j.geomorph.2015.03.040.
- [9] B. Y. C. S. Ummah, Khairul, Sukiyah, Emi, Rosana, Mega Fatimah, Alam, "Remote Sensing Identification of Possible Meteorite Impact Crater on Ciletuh, West Java .," *Int. J. Adv. Sci. Eng. Inf. Technol.*, 8, (5), pp. 1962–1968, 2018, doi: 10.18517/ijaseit.8.5.5559.
- [10] D. P. Leech, P. J. Treloar, N. S. Lucas, & J. Grocott, "Landsat TM analysis of fracture patterns: A case study from the Coastal Cordillera of northern Chile," *Int. J. Remote Sens.*, 24, (19), pp. 3709–3726, 2003, doi: 10.1080/0143116031000102520.
- [11] R. G. Thannoun, "Automatic Extraction and Geospatial Analysis of Lineaments and their Tectonic Significance in some areas of Northern Iraq using Remote Sensing Techniques and GIS," *Int. J. Enhanc. Res. science Technol. Eng.*, 2, (2), pp. 1–11, 2013.
- [12] J. Meixner, J. C. Grimmer, A. Becker, E. Schill, & T. Kohl, "Comparison of different digital elevation models and satellite imagery for lineament analysis: Implications for identification and spatial arrangement of fault zones in crystalline basement rocks of the southern Black Forest (Germany)," *J. Struct. Geol.*, 108, pp. 256–268, 2018, doi: 10.1016/j.jsg.2017.11.006.
- [13] M. Ramdhan *et al.*, "Relocation of hypocenters from DOMERAPI and BMKG networks: a preliminary result from DOMERAPI project," *Earthq. Sci.*, 30, (2), pp. 67–79, 2017, doi: 10.1007/s11589-017-0178-3.
- [14] F. Gob *et al.*, "River responses to the 2010 major eruption of the Merapi volcano, central Java, Indonesia," *Geomorphology*, 273, pp. 244–257, 2016, doi: 10.1016/j.geomorph.2016.08.025.
- [15] D. Gentana, E. Sukiyah, N. Sulaksana, E. T. Yuningsih, & L. Balia, "Determination of Tanggamus Geothermal Prospect Area, Lampung Province, South Sumatra Based on Remote Sensing and 3D Micromine Software," *FIG Work. Week*, 8871, 2017.
- [16] X. Shi & B. Xue, "Deriving a minimum set of viewpoints for maximum coverage over any given digital elevation model data," 8947, (July), 2016, doi: 10.1080/17538947.2016.1207718.
- [17] H. G. Hartono, A. Sudradjat, & O. Verdiansyah, "Caldera of Godean, Sleman, Yogyakarta: A Volcanic Geomorphology Review," *Forum Geogr.*, 31, (1), pp. 139–148, 2017, doi: 10.23917/forgeo.v31i1.2821.
- [18] Suroño, "Litostratigrafi dan sedimentasi Formasi Kebo dan Formasi Butak di Pegunungan Baturagung, Jawa Tengah Bagian Selatan," *Indones. J. Geosci.*, 3, (4), pp. 183–193, 2008, doi: http://dx.doi.org/10.1016/j.ijpe.2010.01.014.
- [19] A. Suroño & Permana, "Lithostratigraphic And Sedimentological Significants Of Deepening Marine Sediments of The Sambipitu Formation Gunung Kidul Residence, Yogyakarta," *Bull. Mar. Geol.*, 26, (1), pp. 15–30, 2009.
- [20] H. Gendoet & B. Sutikno, "Gunungkidul, Yogyakarta," *Indones. J. Geosci.*, 2007.
- [21] R. Gertisser, S. J. Charbonnier, J. Keller, & X. Quidelleur, "The geological evolution of Merapi volcano, Central Java, Indonesia," *Bull. Volcanol.*, 74, (5), pp. 1213–1233, 2012, doi: 10.1007/s00445-012-0591-3.
- [22] H. Rahardjo, Wartono; Sukandarrumidi; Rosidi, "Geological Map of the Yogyakarta Sheet, Java." Geological Research and Development Centre, Bandung, 1995.
- [23] G. M. Buchanan *et al.*, "Free satellite data key to conservation," *Science (80)*, 361, (6398), pp. 139–140, 2018, doi: 10.1126/science.aau2650.
- [24] T. Liu, H. Yan, & L. Zhai, "Extract relevant features from DEM for groundwater potential mapping," in *International Archives of the Photogrammetry, Remote Sensing and Spatial Information Sciences - ISPRS Archives*, 2015, pp. 112–119, doi: 10.5194/isprsarchives-XL-7-W4-113-2015.
- [25] T. Oguchi, T. Aoki, & N. Matsuta, "Identification of an active fault in the Japanese Alps from DEM-based hill shading," *Comput. Geosci.*, 29, (7), pp. 885–891, 2003, doi: 10.1016/S0098-3004(03)00083-9.
- [26] F. Veronesi & L. Hurni, "A GIS tool to increase the visual quality of relief shading by automatically changing the light direction," *Comput. Geosci.*, 74, pp. 121–127, 2015, doi: 10.1016/j.cageo.2014.10.015.
- [27] K. A. Mogaji, O. S. Aboyeji, & G. O. Omosuyi, "Mapping of lineaments for groundwater targeting in the basement complex region of Ondo State, Nigeria, using remote sensing and geographic information system (GIS) techniques," *Int. J. Water Resour. Environ. Eng.*, 3, (7), pp. 150–160, 2011.
- [28] C. L. Salui, "Methodological Validation for Automated Lineament Extraction by LINE Method in PCI Geomatica and MATLAB based Hough Transformation," *J. Geol. Soc. India*, 92, pp. 321–328, 2018, doi: 10.1007/s12594-018-1015-6.
- [29] A. V. Argyriou, R. M. Teeuw, D. Rust, & A. Sarris, "GIS multi-criteria decision analysis for assessment and mapping of neotectonic landscape deformation: A case study from Crete," *Geomorphology*, 253, pp. 262–274, 2016, doi: 10.1016/j.geomorph.2015.10.018.
- [30] K. Pareta & U. Pareta, "Quantitative Morphometric Analysis of a Watershed of Yamuna Basin, India using ASTER (DEM) Data and GIS," *Int. J. Geomatics Geosci.*, 2, (1), pp. 278–284, 2011.
- [31] E. Flores-Prieto, G. Quénéhervé, F. Bachofer, F. Shahzad, & M. Maerker, "Morphotectonic interpretation of the Makuyuni catchment in Northern Tanzania using DEM and SAR data," *Geomorphology*, 248, pp. 427–439, 2015, doi: 10.1016/j.geomorph.2015.07.049.
- [32] L. Guerit, S. Dominguez, J. Malavieille, & S. Castelltort, "Deformation of an experimental drainage network in oblique collision," *Tectonophysics*, 693, pp. 210–222, 2016, doi: 10.1016/j.tecto.2016.04.016.